ohio2/yjy-yjy/yjy-yjy/yjy99907/yjy6390d07z | xppws | 23:ver.3 | 7/17/08 | 19:01 | Msc: jp-2008-03025v | TEID: mac00 | BATID: jp9a210

Linear and Nonlinear Optical Properties of Mesoionic Oxyallyl Derivatives: Enhanced Non-Resonant Third Order Optical Nonlinearity in Croconate Dyes

Ch. Prabhakar,[†,‡] K. Yesudas,[†] K. Bhanuprakash,[*,†] V. Jayathirtha Rao,[*,‡] R. Sai Santosh Kumar,[§] and D. Narayana Rao[*,§]

Inorganic Chemistry Division, Organic Chemistry Division, Indian Institute of Chemical Technology, Hyderabad-500 607, India, and School of Physics, University of Hyderabad, Hyderabad-500 046, India

Received: April 4, 2008; Revised Manuscript Received: June 6, 2008

Role of the donor groups connected to the oxyallyl central moiety (suggested to be a powerful acceptor) has been emphasized in the literature for tuning the absorption maxima and obtaining large NLO activity in croconates and squaraine dyes which are oxyallyl derivatives. Here we have prepared a series of new croconate dye model molecules with aniline and substituted anilines as strong donors to the oxyallyl ring. Using experimental and theoretical techniques like UV−visible spectra, degenerate four wave mixing (DFWM), density functional theory, time-dependent density functional theory, and symmetry adopted cluster-configuration interaction (SAC-CI), we have characterized linear absorption, nonresonant third order optical nonlinearity, charge transfer, and excited states of these molecules. We find that these molecules have smaller singlet diradical character and the absorption is not in the near-infrared (NIR), as other reported croconates, but in the 440−480 nm range. There is a larger charge transfer (CT) from the side groups to the central ring in these croconates evident from SAC-CI calculations compared to CT in NIR croconates. This clearly supports the model that the NIR absorption in oxyallyl derivatives is correlated to the singlet diradical character and not to the donor capacity. The γ values determined by DFWM experiments show large nonresonant values of -2.4 to -5.3×10^{-32} esu, which is larger than that of similar squaraines suggesting that the larger oxyallyl ring size and diradical character in croconates play the major role and not the donor groups. We conclude that with a noncentrosymmetric structure, tunable absorption (visible-NIR), and larger γ values, these less studied croconate dyes are more interesting and will have a major role to play than the widely reported centrosymmetric squaraines as molecular materials.

Introduction

Nonlinear optics (NLO) deals with the interaction of applied electromagnetic fields (like laser light) in various materials to generate new electromagnetic fields altered in frequency, phase, or other physical properties.[1–11] This field has attracted lot of interest in the past two decades not only because of the possible numerous applications in telecommunications, dynamic holography, frequency mixing, optical data storage, and so forth, but also because of the fundamental science connected to issues like charge transfer, conjugation, polarization, and recently suggested diradical character.[12–16] Owing to the combination of chemical tunability, choice of synthetic strategies, and ultrafast response time, organic molecules in particular have received much attention. In fact synthesis, characterization, and modeling of new molecules for second and third order NLO is a very active field.[17–24] For the third order NLO, property of organic molecules studies have been carried out under both resonance and nonresonance conditions with the former yielding values which are 1−2 orders of magnitude larger than the latter.

A widely studied molecular material for the third order NLO is the centrosymmetric squaraine with various substitutions (Scheme 1a).[21] The large third order NLO of these molecules has been attributed to its D-A-D structure with central ring acting as an acceptor due to the two positive charges localized on this ring.[21] It has been proposed that the corresponding croconate dyes (Scheme 1b), which are also derivatives of the oxyallyl substructure like the squaraine, would have a larger acceptance capacity due to the three positive charges localized on the central ring, which in turn should lead to larger NLO activity and the absorption maxima shifted further into the red.[25,26] Two recent studies reported the resonant third order NLO of two NIR croconate dyes and showed that these have an order of magnitude larger NLO activity when compared to the corresponding squaraine dyes.[21] Recently, an oxyallyl-based dye with no central ring, BM4i4i, was reported having an absorption maxima in the NIR and large NLO activity.[20] We carried out high level SAC-CI studies of all these molecules absorbing in NIR and their derivatives and found that there was no large charge transfer from the side groups to the middle central ring.[14a,b,16] We also found that the major transition in these

SCHEME 1: Representative Structures for Squarylium-based and Croconate-based Dyes

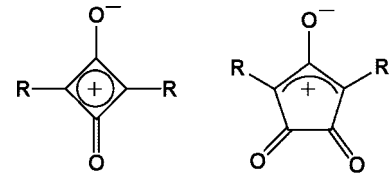

* To whom correspondence should be addressed. E-mail: (K.B.) bhanu2505@yahoo.co.in; (V.J.R.) jrao@iict.res.in; (D.N.R) dnrsp@uohyd.ernet.in.
† Inorganic Chemistry Division, Indian Institute of Chemical Technology.
‡ Organic Chemistry Division, Indian Institute of Chemical Technology.
§ University of Hyderabad.

10.1021/jp803025v CCC: $40.75

SCHEME 2: Reaction Conditions: (a) in MeOH Reflux for 20−50 min

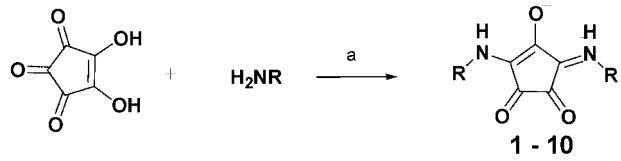

R=

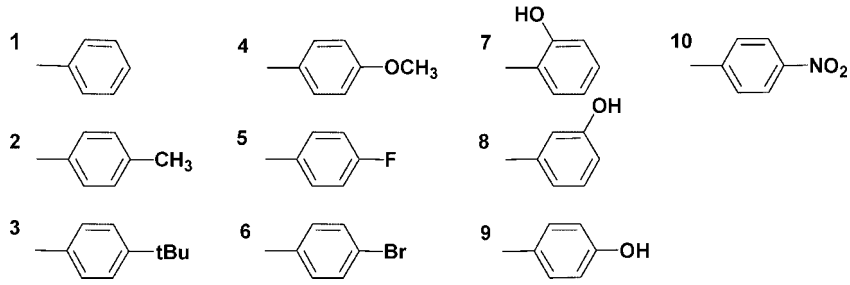

SCHEME 3: Reaction conditions: (i) $NaHCO_3$ + Na_2SO_3 in Distilled H_2O with Aeration 80−90 °C; (ii) MnO_2 in 0.05 M NaOH Reflux for 45 min, Concentrated HCl + $BaCl_2$ in Water at 85−90 °C for 15 min; (iii) 3N H_2SO_4 60−70 °C for 1 hr

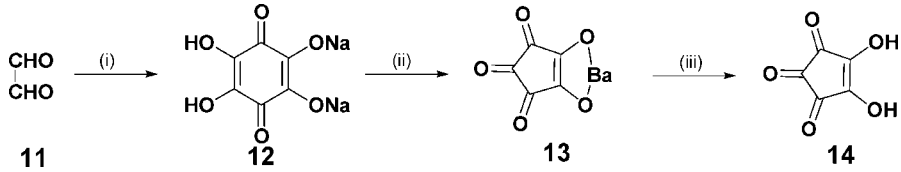

molecules is between the highest occupied molecular orbital (HOMO) to lowest unoccupied molecular orbital (LUMO), which is localized on the oxyallyl moiety. Further, we noticed a correlation of the angle of the central oxyallyl ring and the absorption; the larger the central angle, the larger the bathochromic shift due to smaller HOMO−LUMO gap which arises due to the stabilization of LUMO and destabilization of the HOMO.[15b] Thus, the croconate dyes with a central C−C−C bond angle range of 103−112° have an absorption maxima around 100 nm red-shifted compared to the corresponding squaraine, which has central angle of 87−92°.[16a] An interesting result of this is that lowering of the HOMO−LUMO gap also increases the singlet diradical character as the parent substructure in which oxyallyl is basically a triplet.[14a,c] Thus the diradical character of a croconate dye would be always larger than the corresponding squaraine dye. Further increase in the diradical character in the dyes can be achieved, for example, by increasing the conjugation between the central ring and side groups. We have also shown that there is direct correlation of the diradical character and near-infrared absorption in these molecules.[14a] This is of major interest as molecules with high diradical character have been theoretically shown to have large third order NLO activity.[12,13,15a]

In this work, we report the preparation and characterization of novel croconate dyes. We choose molecules with different donating groups on the side rings varying from unsubstituted molecule 1 to alkyl groups in molecules 2, 3, and 4, halo groups in molecule 5 and 6, hydroxy groups in molecules 7, 8, and 9, and nitro group in molecule 10 (Scheme 2). Here, our aim is to determine the linear and nonlinear properties of these croconates. To the best of our knowledge, no nonresonant measurements of croconate dyes have been carried out, and we expect based on our earlier suggested model that these values would be large.[15a] As mentioned above, the diradical character is correlated to the absorption maxima. These dyes are shown to have around 28% diradical character and the absorption maxima around 440−480 nm. We further carried out third order NLO measurements of these dyes using degenerate four wave mixing (DFWM) techniques and estimated $\chi^{(3)}$. We also obtained from the experiment the molecular level γ of all these molecules by including solvent effects and found them to be large with negative sign. We carried out theoretical studies to determine the origin of the large γ and found that the two state model is sufficient to estimate the major part of the γ in these molecules. We conclude that the absorption is in the visible in spite of the strong donors and larger γ value obtained in these dyes compared to the well-studied squaraine molecules is due to the diradical character in the croconate dye.

Experimental Section

Materials and Instruments. Croconic acid was prepared by the procedure reported in literature (Scheme 3).[27] All other reagents were A.R grade and used without purification. 1H-NMR spectra was recorded on 500 and 200 MHz Spectrophotometers in DMSO with TMS as a standard. IR spectra were taken on a SHIMADZU 435 infrared spectrophotometer. UV−visible absorption spectra were measured on a Jasco V-550 spectrophotometer. Mass spectra were obtained by using electro spray ionization iontrap mass spectrometry (Thermofinnigan, Sanzox, CA, USA). High resolution mass spectra (HRMS) were carried out by using electro spray ionization quadruple time-of-flight (ESI Q Tof) mass spectrometry (QSTAR XL, Applied biosystems/MSD sciex, Fostercity, USA).

The third order nonlinear optical studies were carried out by the DFWM studies. Ultrashort laser pulses used in the present study were obtained from a conventional chirped pulse amplification (CPA) system comprising of an oscillator (Maitai, Spectra-Physics Inc.) that delivers an ∼80 fs, 82 MHz pulse train with pulse energy of 1 nJ at 800 nm and a regenerative

ohio2/yjy-yjy/yjy-yjy/yjy99907/yjy6390d07z | xppws | 23:ver.3 | 7/17/08 | 19:01 | Msc: jp-2008-03025v | TEID: mac00 | BATID: jp9a210

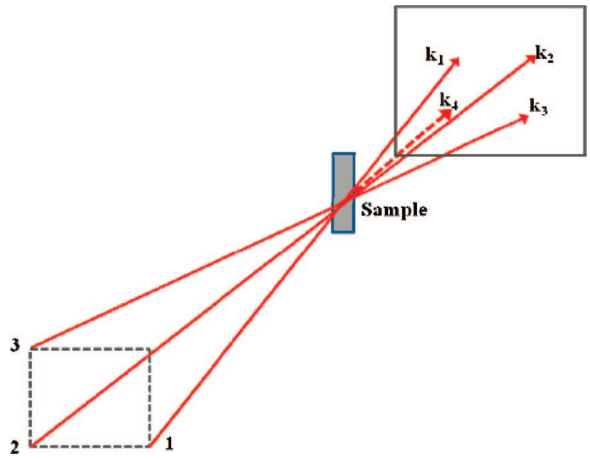

Figure 1. Geometry of the DFWM experiment. Beams 1−3 are coincident on the sample. The resultant fourth beam (dashed) is the DFWM signal that occurs because of the interaction $k_4 = k_3 - k_2 + k_1$.

amplifier (Spitfire, Spectra Physics Inc.), pumped by a 150 ns, 1 kHz, Q-switched Nd:YLF laser. After regenerative amplification, we obtained amplified pulses of pulse width ∼100 fs determined by second order intensity autocorrelation with output energy of up to 1 mJ at 1 kHz repetition rate. The DFWM setup used was in box-car geometry.[7b] In brief, in a box-car arrangement the fundamental beam is divided into three nearly equal intensity beams in such a way that the three form three corners of a square box and are focused into the nonlinear medium (sample) both spatially and temporally. The resultant DFWM signal comes as the fourth corner of the box generated as a result of the phase-matched interaction $k_4 = k_3 - k_2 + k_1$ of the three incident beams as shown in the Figure 1. The sample under consideration is taken in the form of solution filled in a 1 mm glass cuvvette. Care was taken to reduce the contribution of the cuvvette toward the overall DFWM signal by choosing suitable focusing conditions. By maintaining same polarization for the three incident beams we estimated $\chi^{(3)}_{1111}$. A half-wave plate was introduced in the path of beam-2 to have its polarization perpendicular to that of beam-1 and beam-3 so that we could estimate $\chi^{(3)}_{1212}$. The transient DFWM profiles for the sample were obtained by delaying the beam-3 with respect to the other two incident beams. By performing the nonlinear transmission experiments on the sample, the input powers for the three input pulses were chosen such that effect of nonlinear absorption can be neglected, and hence the obtained DFWM signal contains purely instantaneous nonlinear response of the sample. The obtained $\chi^{(3)}$ data is purely real in nature without any contribution of imaginary components due to multiphoton absorption. Also, the choice of low input powers allows us to neglect the contribution of higher order nonlinearities. Since all the samples show no absorption at the laser wavelength (800 nm), we expect $\chi^{(3)}$ and γ values are nonresonant.

Synthesis and Characterization

General Procedure for the Preparation of 1,3-Disubstituted Croconates (Molecules 1−10) (Scheme 2). Croconate dyes are synthesized by taking 2.1 mMol (300 mg) of croconic acid dissolved in 10 mL of MeOH; to this solution 4.2 mMol of substituted aniline (1:2 ratio) was added at 60 °C. Reaction mixture was refluxed for 20−50 min. The precipitated solid was filtered through Buckner funnel and washed with MeOH (10 mL portions 3 times). Yield: 60−70%.[28]

(1) 1,3-Bis(anilino) Croconate. Yield 60%; mp 286−288 °C. ^{1}H NMR (DMSO) δ: 7.2 −7.6 (m, 10H), 11.5 (b, 2H). MS (ESI): m/z 292.8 $(M + H)^+$. IR (KBr): 3170 cm^{-1} (NH), 1711 and 1661 cm^{-1} (C═O), 1447 cm^{-1} (C−N). HRMS (m/z): [M + Na] for $C_{17}H_{12}N_2O_3Na$ calcd for $C_{17}H_{12}N_2O_3Na$, 315.0745; found, 315.0756.

(2) 1,3-Bis(4-toluedeno) Croconate. Yield 64%; mp 295−297 °C. ^{1}H NMR (DMSO) δ: 7.2−7.4 (m, 8H), 11.4 (b, 2H), 2.3(s, 6H). MS (ESI): m/z 321 $(M + H)^+$. IR (KBr): 3168 cm^{-1} (NH), 1709 and 1660 cm^{-1} (C═O), 1462 cm^{-1} (C−N). HRMS (m/z): [M + Na] calcd for $C_{19}H_{16}N_2O_3Na$, 343.1058; found, 343.1064.

(3) 1,3-Bis(4-*t*-butylanilino) Croconate. Yield 64%; mp 280−283 °C. ^{1}H NMR (DMSO) δ: 7.3−7.6 (m, 8H), 1.3 (s, 18H). MS (ESI): m/z 405.1 $(M + H)^+$. IR (KBr): 3437 cm^{-1} (NH), 1703 and 1650 cm^{-1} (C═O), 1425 cm^{-1} (C−N). HRMS (m/z): [M + Na] calcd for $C_{25}H_{28}N_2O_3Na$, 427.1997; found, 427.1996.

(4) 1,3-Bis(4-anisidino) Croconate. Yield 65%; mp 282−283 °C. ^{1}H NMR (DMSO) δ: 6.8 (d, 2H), 6.9 (d, 2H), 7.0 (d, 2H), 7.2 (d, 2H), 3.8 (s, 6H). MS (ESI): m/z 352.6 $(M + H)^+$. IR (KBr): 3185 cm^{-1} (NH), 1708 and 1650 cm^{-1} (C═O), 1426 cm^{-1} (C−N). HRMS (m/z): [M + Na] calcd for $C_{19}H_{16}N_2O_5Na$; 375.0956; found, 375.0968.

(5) 1,3-Bis(4-fluroanilino) Croconate. Yield 60%; mp 271−274 °C. ^{1}H NMR (DMSO) δ: 7.0 − 7.6 (m, 8H). MS (ESI): Neg. mode m/z 327.2 $(M - H)^+$. IR (KBr): 3182 cm^{-1} (NH), 1703 and 1608 cm^{-1} (C═O), 1436 cm^{-1} (C−N). HRMS (m/z): [M + Na] calculated for $C_{17}H_{10}N_2O_3F_2Na$, 351.0557; found, 351.0552.

(6) 1,3-Bis(4-bromoanilino) Croconate. Yield 67%; mp >300 °C. ^{1}H NMR (DMSO) δ: 7.4 (d, 4H), 7.6 (d, 4H). MS (ESI): m/z 448.5, 450.5 and 452.5 in 1:2:1 ratio $(M + H)^+$. IR (KBr): 3179 cm^{-1} (NH), 1706 and 1628 cm^{-1} (C═O), 1486 cm^{-1} (C−N). HRMS (m/z): [M + Na] calcd for $C_{17}H_{10}N_2O_3Br_2Na$, 470.8955; found, 470.8977.

(7) 1,3-Bis(2-aminophenol) Croconate. Yield 66%; mp 205−207 °C. ^{1}H NMR (DMSO) δ: 6.8- 7.3 (m, 8H), 7.5 (b,1H), 10.3 (b, 1H), 10.7 (b, 2H). MS (ESI) m/z 325 $(M + H)^+$. IR (KBr): 3216 cm^{-1} (NH), 1702 and 1619 cm^{-1} (C═O), 1424 cm^{-1} (C−N). HRMS (m/z): [M + Na] calcd for $C_{17}H_{12}N_2O_5Na$, 347.0643; found, 347.0640.

(8) 1,3-Bis(3-aminophenol) Croconate. Yield 76%; mp 193−195 °C. ^{1}H NMR (DMSO) δ: 6.60−7.2 (m, 8H), 9.7 (b, 2H). MS (ESI) m/z 325 $(M + H)^+$. IR (KBr): 3184 cm^{-1} (NH), 1710 and 1595 cm^{-1} (C═O), 1481 cm^{-1} (C−N). HRMS (m/z): [M + Na] calcd for $C_{17}H_{12}N_2O_5Na$, 347.0643; found, 347.0655.

(9) 1,3-Bis(4-aminophenol) Croconate. Yield 73%; mp >300 °C. ^{1}H NMR (DMSO) δ: 6.8 (d, 4H), 7.4 (m, 4H), 9.8 (s, 2H), 11.3(s, 2H). MS (ESI) m/z 324.9 $(M + H)^+$. IR (KBr): 3068 cm^{-1} (NH), 1700 and 1609 cm^{-1} (C═O), 1430 cm^{-1} (C−N). HRMS (m/z): [M + Na] calcd for $C_{17}H_{12}N_2O_5Na$, 347.0643; found, 347.0659.

(10) 1,3-Bis(4-nitroanilino) Croconate. Yield 64%; mp 288−290 °C. ^{1}H NMR (DMSO) δ: 6.7 (d, 2H), 7.4 (d, 2H), 8.0 (d, 2H), 8.2 (d, 2H), 10.1 (b, 2H). MS (ESI): m/z 382.9 $(M + H)^+$. IR (KBr): 3285 cm^{-1} (NH), 1708 and 1672 cm^{-1} (C═O), 1445 cm^{-1} (C−N). HRMS (m/z): [M + Na] calcd for $C_{17}H_{10}N_4O_7Na$, 421.0186; found, 421.0179.

Computational Studies. In this study, all the calculations have been carried out using Gaussian 03 ab initio/DFT quantum chemical package.[29] The atomic positions of the molecules in all possible geometrical conformations were fully relaxed by Berny optimization algorithm at DFT-B3LYP with 6-31G(d,p) basis set with a default integration grid. The theoretical singlet equilibrium structures were obtained when the maximum internal forces acting on all the atoms and the stress were less

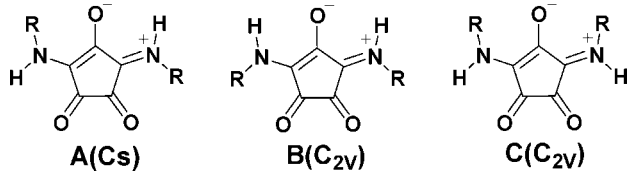

Figure 2. Geometrical conformations of croconates.

than 4.5×10^{-4} eV/Å and 1.01×10^{-3} kBar, respectively, which were further confirmed by vibrational analysis. To check the numerical consistency in the basis set, we further relaxed the minimal equilibrium conformation obtained at 6-31G(d,p) level with 6-311+G(d,p) basis set with symmetry constraint, and we observed a maximum difference of 0.007 Å in bond lengths and 0.4° in bond angles. Because of this small difference in geometries, it is confirmed that we reached the consistency within the basis set limit of 6-31G(d,p). Therefore, we carried out further calculations of molecular properties with the 6-31G(d,p) equilibrium minimal geometries. Time-dependent density functional theory (TDDFT)[30] studies have been carried out to estimate the lowest five singlet−singlet transitions at the same basis set level both in vacuo and in solvent media ($CHCl_3$ and DMF). We have also calculated the nonlinear second hyperpolarizabilities (γ) using the TDDFT within the three-state model.

Symmetry adopted cluster/symmetry adopted cluster-configuration interaction (SAC/SAC-CI)[31,15b] calculations to understand charge transfer (CT) in the ground and first excited-state in molecule 1 are carried out at level two with an active space of 161 orbitals in which 41 occupied and 120 unoccupied orbitals at 6-31G(d, p) basis with default convergence criteria using the geometry obtained at B3LYP/6-31G(d, p) level. The details of SAC/SAC-CI calculations are shown in Supporting Information.

Results and Discussions

Molecular Structures, Geometries, and Dipole Moments. As our main aim is determining the molecular NLO property γ and its variation with substitutions for these croconate dyes, it would be of interest to predict the conformations, geometry, ground-state dipole moments, and subsequently the transition dipole moments of the major transition of the molecules both in solvent and gas phase using quantum chemical methods. We notice that there are three major possible planar conformations for the molecules as shown in Figure 2. Conformation A, which is essentially a trans geometry, has the lowest symmetry, C_s, whereas B and C have higher symmetry, C_{2v}/C_2. In the case of molecule 8 only there are many more low lying conformations due to the OH group at 3-position in addition to these three major conformations. The details of the geometrical parameters of the central ring of all the molecules, their conformations, and relative energies obtained at the B3LYP/6-31G (d,p) level are indicated in the Figure 3 and Table 1, respectively. For clarity, we have indicated only the range in Figure 3(for conformation B only), and it is very clear that the geometrical parameters of the central ring hardly vary with substitutions. This is an important observation as we have shown in the earlier studies using quantum chemical principles that in the oxyallyl derivatives the first excited-state is basically a HOMO−LUMO transition which is localized on the central ring.[15b,16a]

From Table 1, it is clearly seen that the relative energy differences for all the molecules in the gas phase between conformations A, B, and C are less than 2.0 kcal/mol, while between A and B it is around 1 kcal/mol. The most stable conformation in the gas phases for most of the molecules is A, except in molecule 8 where B is the more stable. We have also carried out the calculation of the relative energies in the solvent phase. The relative energies change slightly with now both A and B conformation being almost degenerate in the more polar solvent, while in 2−3 cases the conformation B becomes more stable. Conformer C is slightly higher in energy. The dipole moments obtained in the gas phase for the different conformations are shown in the same Table. It is quite large for conformation B, in molecule 10 which is NO_2 substituted but slightly lower in the other conformations. On the other hand the unsubstituted molecule 1 has nearly same dipole moment in all the three conformations. In molecules with donor groups 2−4, the dipole moments of B are slightly lower. In the case of molecules with OH groups, the dipole moment of conformation A is also quite large except in the case of molecule 7. It is expected that those conformations with larger dipole moments

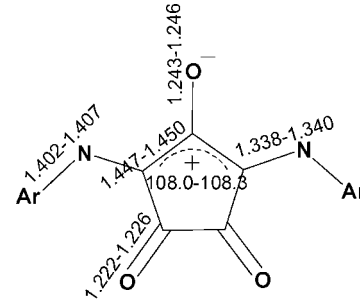

Figure 3. Selected optimized bond lengths (in Ångstroms) and angle (in degrees) of the B-conformation of all the molecules obtained at B3LYP/6-31G(d,p) level of theory (only the range given).

TABLE 1: Relative Energies (in kcal/mol) Calculated in Gas Phase and Solvents for Different Conformations for Molecules 1−10 at B3LYP/6-31G(d,p) Level of Theory[a]

		relative energy		
molecule	conformation	gas phase	$CHCl_3$	DMF
1	A	0.0(3.8)	0.0	0.0
	B	1.0(3.8)	0.5	0.1
	C	1.4(3.7)	1.8	1.8
2	A	0.0(4.1)	0.0	0.0
	B	1.0(3.6)	0.5	0.1
	C	1.4(4.5)	1.7	1.7
3	A	0.0(4.1)	0.0	0.1
	B	1.0(3.5)	0.2	0.0
	C	1.4(4.7)	1.7	1.8
4	A	0.0(4.2)	0.0	0.0
	B	0.9(1.2)	0.4	0.1
	C	1.7(3.6)	1.9	1.9
5	A	0.0(3.4)	0.0	0.0
	B	1.0(4.4)	0.5	0.0
	C	1.3(1.8)	1.7	1.8
6	A	0.0(2.7)	0.0	0.0
	B	1.0(4.4)	0.4	0.0
	C	1.4(1.2)	1.7	1.8
7	A	0.0(4.8)	0.0	0.0
	B	0.8(5.6)	0.5	0.3
	C	0.8(3.8)	0.5	1.3
8	A	0.7(2.9)	0.0	0.0
	B	0.0(3.6)	0.0	0.0
	C	1.2(2.9)	2.9	2.0
9	A	0.0(3.8)	0.0	0.1
	B	0.9(1.2)	0.3	0.0
	C	2.0(2.6)	2.0	1.9
10	A	0.0(1.5)	0.0	0.0
	B	1.1(5.4)	0.5	0.0
	C	1.3(3.8)	1.7	1.7

[a] The values given in parenthesis correspond to Dipole moments (μ in Debye) in gas phase.

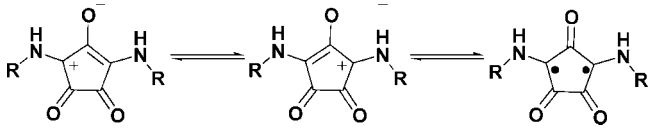

Figure 4. Schematic representations of resonance forms of croconates.

TABLE 2: HOMO-LUMO Gap (HLG in eV), Singlet-Triplet Gap ($\Delta E_{S\text{-}T}$ in kcal/mole) obtained at B3LYP/6-31G(d,p) Level[a]

molecule	HLG	$\Delta_{S\text{-}T}$	% *Yi*
1	2.35	21.1	28.1
2	2.32	20.8	28.4
3	2.32	20.9	28.2
4	2.23	20.3	28.4
5	2.33	20.9	28.4
6	2.29	20.7	28.6
7	2.29	20.5	28.7
8	2.31	20.7	28.1
9	2.25	20.3	28.5
10	2.26	20.5	28.8

[a] Percent diradical character (% Y_i) obtained at UHF/6-31+G(d,p) level.

would be stabilized in polar solvents. For clarity and because of the near degeneracy of A and B conformations in solvents, from now on we discuss the properties of the more symmetric conformation B which is in C_{2v}/C_2 point group.

These molecules are derivatives of oxyallyl subgroup, which is a triplet, and thus retain some amount of varying diradical character. In fact, these can be represented by the resonance structure shown in Figure 4. The amount of % diradical character in each molecule can be estimated by using the method suggested by Nakano et.al.[12,13] The diradical character calculated by this method is tabulated in the Table 2 for the gas phase conformation B. For these molecules, we also calculate the singlet−triplet gap. The values are also shown in the same table. The diradical character is around 28%, which is small to intermediate range, while the singlet−triplet gap is around 20 kcal/mol; this is in good agreement with the diradical character.[32] The HOMO−LUMO gaps obtained for these molecules are also shown in the same table.

Electronic Absorption Spectrum (Linear Optical Properties). We have carried out the UV−vis spectrum analysis of all these compounds in pure DMF and $CHCl_3$. Only three of the compounds (2, 3, and 4) dissolved completely in $CHCl_3$, while the other 7 compounds have been made soluble by adding few drops of DMSO. The experimentally determined spectra is shown in Figure 5, while λ_{max} and ϵ obtained in both DMF and $CHCl_3$ are tabulated in the Table 3. Except for the unsubstituted molecule 1 and F− substituted molecule 5, all the other molecules absorb within the range of 503−522 nm in $CHCl_3$. These two molecules absorb in the range of 485−492 nm. There is only small variation in the absorption maxima with change in groups. There is a small negative solvatochromic effect seen in the absorption maxima when the solvent is changed from $CHCl_3$ to DMF. Here the maximum absorption is only 490 nm while the minimum is 441 nm for 5. The negative solvatochromic effect clearly indicates the stabilization of the zwitterions (Figure 4) in DMF in these molecules. The largest observed shift is in 4 with a change of 55 nm, while the least is for 10 with shift of only 27 nm.

To have a deeper understanding of the observed spectra, we have carried out TDDFT studies including the solvent effect for these molecules. The values obtained are tabulated in Table

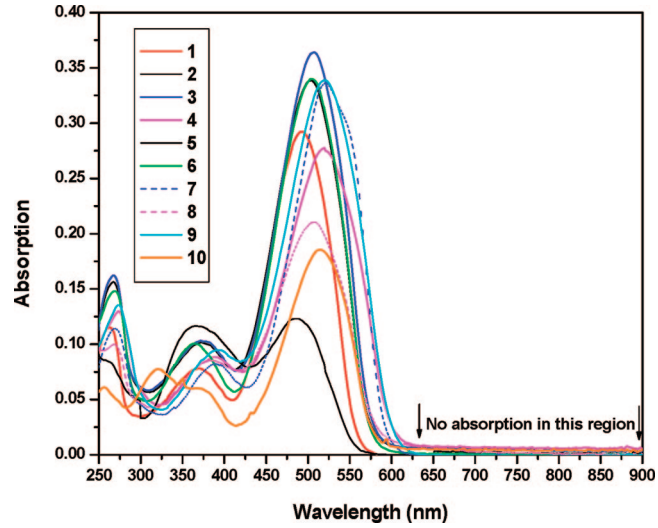

Figure 5. UV−vis absorption spectra of Croconate dyes 1−10 in $CHCl_3$.

TABLE 3: Absorption Maxima (λ_{max} in nm), Absorption Energies (Δ in eV) and Extinction Coefficients (ϵ) in for Molecules 1−10 in Chloroform ($CHCl_3$) and Dimethylformamide (DMF)

	$CHCl_3$		DMF	
molecule	λ_{max} in nm[a]	ϵ at λ_{max} ($\times 10^4$ M^{-1} cm^{-1})	λ_{max} in nm[a]	ϵ at λ_{max} ($\times 10^4$ M^{-1} cm^{-1})
1	492(2.52)	3.40	457(2.71)	3.45
2	504(2.46)	3.94	460(2.70)	2.60
3	507(2.45)	4.23	462(2.68)	2.33
4	517(2.40)	3.23	462(2.68)	1.92
5	485(2.56)	1.43	441(2.81)	2.54
6	504(2.45)	3.96	463(2.68)	3.01
7	521(2.38)	3.91	477(2.60)	2.43
8	507(2.45)	2.45	453(2.74)	2.69
9	521(2.38)	3.94	465(2.67)	2.58
10	515(2.41)	2.16	488(2.54)	3.40

[a] Absorption energies are given in parentheses.

TABLE 4: Calculated Absorption Energies (Δ_{cal} in eV), Oscillator Strength (*f*), Transition Dipole Moments (μ_{ge} in Debye) of all Molecules in Different Solvents obtained at B3LYP/6-31G(d,p) level

	$CHCl_3$			DMF		
molecule	Δ_{cal}	*f*	μ_{ge}[a]	Δ_{cal}	*f*	μ_{ge}[a]
1	2.37	1.125	11.20	2.41	1.114	11.05
2	2.31	1.252	11.95	2.35	1.246	11.82
3	2.31	1.351	12.42	2.34	1.351	12.33
4	2.20	1.322	12.58	2.24	1.307	12.42
5	2.34	1.145	11.35	2.39	1.134	11.19
6	2.28	1.350	12.48	2.33	1.335	12.30
7	2.27	1.135	11.48	2.29	1.109	11.31
8	2.30	1.105	11.25	2.34	1.080	11.03
9	2.22	1.272	12.29	2.25	1.255	12.14
10	2.19	1.345	12.72	2.21	1.343	12.64

[a] On the long axis.

4. The transition dipole moments between the ground-state A_1 to the excited-state B_2 are also tabulated. The major transitions at the orbital level in all the molecules are observed to be HOMO−LUMO, which is localized on the central ring. The MO picture for one of the molecules is shown in Figure 6. The transition dipole moments for the first vertical excitation lie on Y-axis (B_2/B symmetry), which is perpendicular to the permanent dipole moment vector which lies along the central C═O

ohio2/yjy-yjy/yjy-yjy/yjy99907/yjy6390d07z | xppws | 23:ver.3 | 7/17/08 | 19:01 | Msc: jp-2008-03025v | TEID: mac00 | BATID: jp9a210

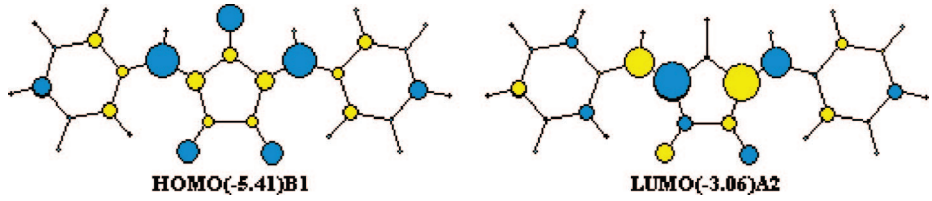

Figure 6. Frontier one electron molecular orbitals of molecule 1.

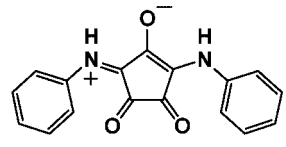

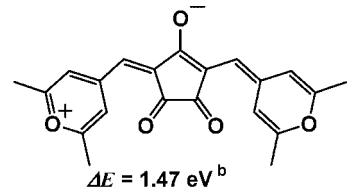

ΔE = 2.52 eV [a] (2.48 eV) [c]

ΔE = 1.47 eV [b] (1.58 eV) [c]

	Ground	Excited	Gain/Loss	Ground	Excited	Gain/Loss
Central ring	0.14	0.02	0.12	-0.17	-0.75	-0.03
Side groups	-0.14	-0.02	-0.12	0.17	0.75	0.03

[a] This work
[b] Reference 33.
[c] SAC-CI results

Figure 7. Comparison of charge transfer (in e) from ground (S_0) to first excited (S_1) states of croconates absorbing in visible and NIR regions.

bond. The transition dipole moments magnitude is quite large, and they lie in the range of 11.2 D−12.7 D. There is a negative solvatochromic effect predicted by calculations also, though the shifts are slightly smaller they are within the predictive accuracy of the TDDFT methodology.[30]

To understand the CT in the first excited-state transition, we analyze the Mulliken π-charge distributions in one of the molecule (molecule 1) 2R and in the central croconate ring (C_5O_3) at SAC/SAC-CI level as shown in Figure 7. We also carried out comparison with an earlier reported croconate absorbing in the NIR region at the same level of SAC/SAC-CI.[33] It is observed that there is a charge donation of 0.12 e from 2R to C_5O_3 groups in the former, while in the latter a maximum of only 0.03 e charge donation from the side groups to the central ring is seen. We again note that there is no correlation to the CT and absorption maxima.[16a]

Third Order Nonlinear Studies. The third order NLO, $\chi^{(3)}$ is obtained by comparing the measured DFWM signal for the sample with that of DMF as reference ($\chi^{(3)} = 4.4 \times 10^{-14}$ esu) under the same experimental conditions. The following relationship is used.

$$\chi^{(3)}_{\text{sample}} = \left(\frac{n_{\text{sample}}}{n_{\text{ref}}}\right)^2 \left(\frac{I_{\text{sample}}}{I_{\text{ref}}}\right)^{1/2} \left(\frac{L_{\text{ref}}}{L_{\text{sample}}}\right) \alpha L_{\text{sample}} \times \left(\frac{e^{\alpha L_{\text{sample}}/2}}{1 - e^{-\alpha L_{\text{sample}}}}\right) \chi^{(3)}_{\text{ref}} \quad (1)$$

where I is the DFWM signal intensity, α is the linear absorption coefficient, L is sample path length, and n is the refractive index. The concentration of sample is very low in solution, so we have taken the refractive index of DMF ($n = 1.431$) as the refractive index of solution. The $\chi^{(3)}$ is estimated in DMF at concentration 5×10^{-5} M. The $\chi^{(3)}$ values at this concentration are tabulated in Table 5. $\chi^{(3)}$ has three independent components namely $\chi^{(3)}_{1111}$, $\chi^{(3)}_{1212}$, and $\chi^{(3)}_{1122}$ in an isotropic medium. In the case of nonresonant electronic NLO, $\chi^{(3)}_{1111} = 3\chi^{(3)}_{1212} = 3\chi^{(3)}_{1122}$ when the three input beams are all vertically polarized, then the corresponding $\chi^{(3)}$ obtained would be $\chi^{(3)}_{1111}$. To determine $\chi^{(3)}_{1212}$, the probe beam is orthogonally polarized with respect to the two pump beams. The ratio of $\chi^{(3)}_{1111}$ to $\chi^{(3)}_{1212}$ should be close to 3 (suggesting that there is no significant contribution arising from the coherent coupling effects).[21d] Here for all samples, we obtain values close to 3(2.7 to 2.9). To rule out the contribution of two-photon absorption to the measured values of $\chi^{(3)}$, we carried out the nonlinear transmittance measurements and input intensity dependent study of the obtained DFWM signal as a function of intensity of the three interacting laser pulses. As shown in Figure 8a for molecule 1 and other molecules in Supporting Information, we obtained a slope of ~3 for all of the samples studied indicating that origin of DFWM does not have contribution from any two-photon absorption in which case the slope of the curve would have been different from 3.[36,37] Figure 8b shows the linearity in the transmission versus the input intensity for the range of intensities from 7×10^9 until 2.7×10^{11} W/cm^2. The DFWM signal was measured at 1.7×10^{10} W/cm^2, which is well below the appearance of nonlinear absorption. From Figure 8, we can conclude that the linear absorption is negligible and TPA can appear only at very high intensities well above

TABLE 5: Measured Third-Order Nonlinear Susceptibility ($\chi^{(3)}$), Second Order Hyperpolarizability (γ_{obs} in esu) for Molecules 1−10, Obtained from DFWM Technique in Dimethyformamide Solution[a]

molecule	$\chi^{(3)}$ ($\times 10^{-14}$ in esu)	γ_{obs} ($\times 10^{-32}$ in esu)	γ_{calc} ($\times 10^{-32}$ in esu)
1	4.1	−2.4	−0.6
2	4.1	−3.3	−0.9
	(3.6)[b]	(−3.5)[b]	(−1.0)
3	4.1	−3.2	−1.1
	(3.7)[b]	(−2.5)[b]	(−1.1)
4	4.1	−3.1	−1.2
	(3.6)[b]	(−3.7)[b]	(−1.4)
5	3.9	−4.2	−0.7
6	3.9	−3.8	−1.1
7	4.0	−4.1	−0.8
8	3.9	−3.8	−0.7
9	4.1	−3.6	−1.1
10	3.8	−5.3	−1.4

[a] Calculated second order hyperpolarizability(γ_{calc} in esu) obtained by two state model using TDDFT-B3LYP/6-31G(d,p) level including solvent effects. [b] Values given in parenthesis are measured in $CHCl_3$.

ohio2/yjy-yjy/yjy-yjy/yjy99907/yjy6390d07z | xppws | 23:ver.3 | 7/17/08 | 19:01 | Msc: jp-2008-03025v | TEID: mac00 | BATID: jp9a210

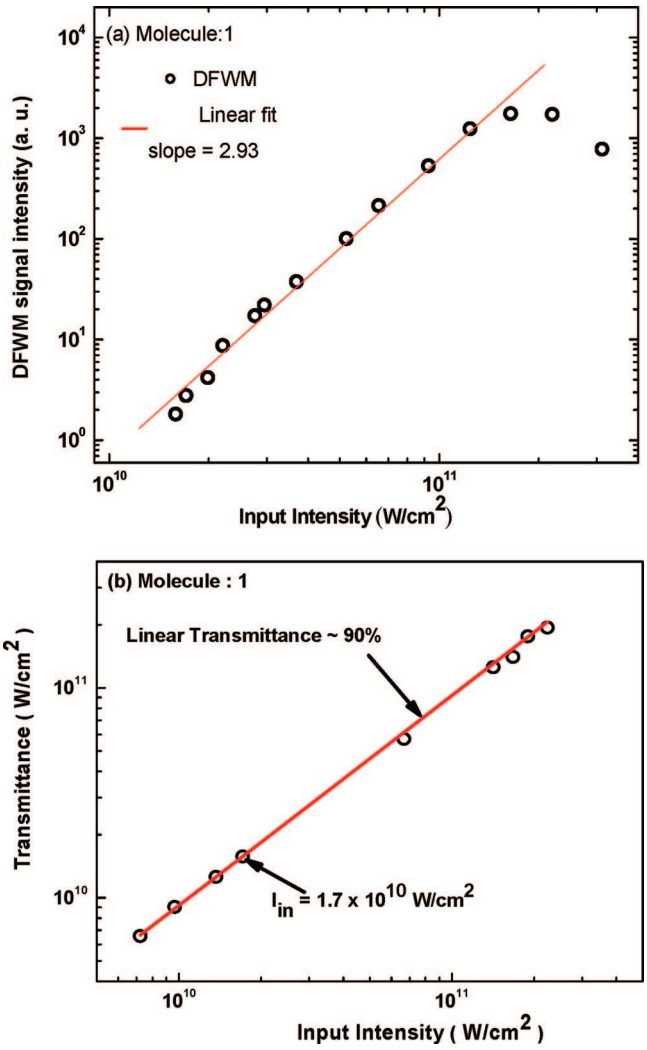

Figure 8. (a) Plots showing the cubic dependence of DFWM as a function of input intensity. (b) Plot of output transmittance vs input power.

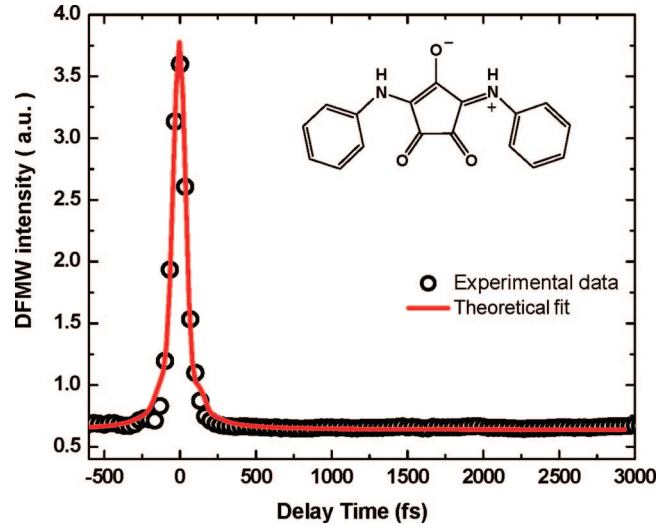

Figure 9. Temporal profiles of DFWM signal of the molecule 1 in DMF (concentration: 5×10^{-5} M) as a function of beam 3 delay time for the parallel configurations.

the intensities (indicated by arrow in Figure 8b) used for the measurement of $\chi^{(3)}$. Therefore the measured values of $\chi^{(3)}$ can be taken as dominant nonresonant.

The $\chi^{(3)}$ values vary from 3.8×10^{-14} to 4.1×10^{-14} esu and are quite large. The temporal response for molecule 1 is shown in Figure 9, the nonlinear responses are very fast and are of the order of 100 fs (for other molecules see Supporting Information). We also carried out the determination of $\chi^{(3)}$ value at the same concentration for three samples(2, 3 and 4) which are completely soluble in chloroform ($n = 1.460$). These values are shown in the same table and are found to be quite large.

To estimate the γ value at the molecular level we use the following formula

$$\chi^{(3)}_{\text{sample}} = \left(\frac{n^2+2}{3}\right)^4 [N_{\text{solvent}}\gamma_{\text{solvent}} + N_{\text{sample}}\gamma_{\text{sample}}] \quad (2)$$

where n is the refractive index, N is the number density, and γ is the second hyperpolarizability. We carry out the determination of $\chi^{(3)}$ as a function of concentration (1×10^{-5} to 10×10^{-4} M). We see from the plots $\chi^{(3)}$ versus concentration a linear decrease with a negative slope (decreasing $\chi^{(3)}$ with increasing solute concentration) indicates that the γ value would be of negative sign (shown in Figure 10a). The γ values obtained using a linear fit of the above equation is shown in the Table 5 and all these values are negative. In comparison to the unsubstituted molecule 1, molecule 10 with nitro group on the side rings show larger γ. This can be attributed to the larger individual contributions from the side rings to γ. We also carried out the γ value determination of the three samples (2, 3, and 4) in $CHCl_3$. The plot is given in Figure 10b, while the γ values are shown in the same table. They are almost similar to the values obtained in DMF.

To understand the factors responsible for the large γ value, we carry out theoretical analysis of these molecules using quantum chemical methods. It should be kept in mind that our aim is not to determine total γ through computational methods but we are only looking at the component originating due to the central oxyallyl ring. The rest of the γ which we are not calculating originates from the side groups and higher states. The general theoretical background is given below.

The equation for the longitudinal γ (which is the largest based on symmetry) can be written using perturbation theory and sum over state (SOS) as

$$\gamma_{iiii} = 24\sum_{n\neq g}\left[\frac{(\mu^i_{ng}\Delta\mu^i_{ng})^2}{(E_{ng})^3} - \frac{(\mu^i_{ng})^4}{(E_{ng})^3} + \sum_{m\neq n,g}\frac{(\mu^i_{ng})(\mu^i_{nm})^2}{(E_{ng})^2 E_{mg}}\right] \quad (3)$$

where i= x, y, z. Here the parameters μ_{ng}, and μ_{nm}, corresponds to the transition moments between the ground and the n^{th} excited state, and n^{th} excited to m^{th} excited states. $\Delta\mu_{ng}$ is the difference in dipole moments between the ground and the n^{th} excited states. Similarly E_{ng} and E_{mg} correspond to the energy of transition between the ground and the n/m^{th}-excited-state and transition energy between excited states.[34]

In the three state model approximation (ground (A), excited state (B) and the final state (A))[35] and using the symmetry arguments (like $\Delta\mu ng^y$ is zero), we obtain only the following longitudinal major component for our case here,

$$\gamma_{yyyy} = 24\sum_{n\neq g}\left[-\frac{(\mu^y_{1B_2,A_1})^4}{(E_{1B_2,A_1})^3} + \sum_{m\neq n,g}\frac{(\mu^y_{1B_2,A_1})(\mu^y_{2A_1,1B_2})^2}{(E_{1B_2,A_1})^2 E_{2A_1,1A_1}}\right] \quad (4)$$

or in other words $\gamma^T = \gamma^2 + \gamma^3$ where the negative term in the above equation is γ^2 and the positive term is γ^3. In the above expression if the first term dominates, then a negative value is obtained and if second term dominates, a positive value is obtained. From the equation it is also clear that when the

ohio2/yjy-yjy/yjy-yjy/yjy99907/yjy6390d07z | xppws | 23:ver.3 | 7/17/08 | 19:01 | Msc: jp-2008-03025v | TEID: mac00 | BATID: jp9a210

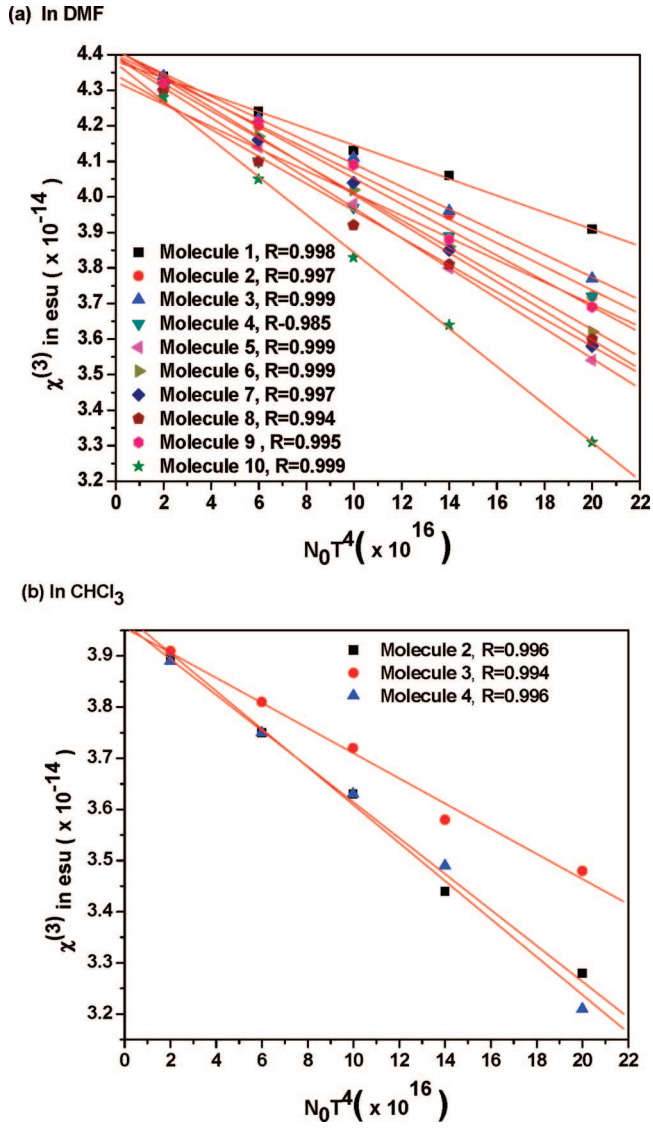

Figure 10. Plots of concentration dependence on $\chi^{(3)}$, (a) in DMF for molecules 1−10 and (b) in $CHCl_3$ for molecules 2, 3 and 4.

transition dipole moment is large and the transition energy is small the γ^2 value increases.

We use this SOS three state model for determining the second order hyperpolarizability of these molecules. We had in our earlier work found that the transition dipole of the excited state to the final excited-state is very small hence; γ^3 can be neglected.[15a] So we use only the two state model which is basically the first term in the above equation. We evaluate the γ for each molecule using the transition dipole moment and the excitation energy obtained in DMF by TDDFT. These are tabulated in the Table 5. The γ is also very large (−0.6 to −1.4 $\times$ 10^{-32} esu) indicating that this central ring in each molecule contributes a large value to the total γ.

Excitation energy of the ground state to B_2 (B_{2U}) states of a simple croconate and the corresponding squaraine is compared in Figure 11. The states have been obtained at the TDDFT-B3LYP/6-31G(d,p) level. It is clearly seen in this correlation diagram due to the widening of angle in croconate all B_2 states become lower in energy with respect to the ground-state when compared to the corresponding squaraines. This is the main cause of larger γ value in croconates.

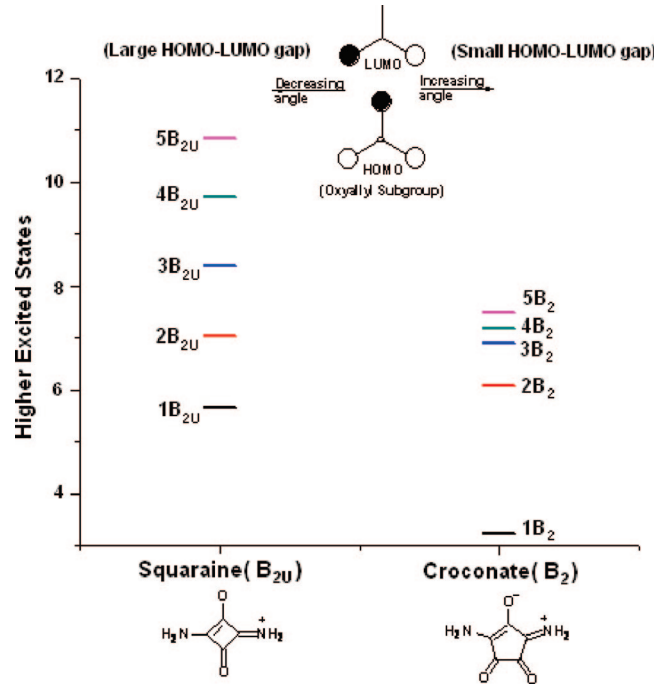

Figure 11. Comparison of B_2/B_{2U} states of simple croconate and squaraine dyes with respect to their ground states.

Conclusions

Though squaraines and croconate dyes are derivatives of oxyallyl subgroup, both have interesting and different properties. Croconate dyes for example have a bathochromic shift of ∼100 nm of the absorption maxima when compared to the corresponding squaraine dyes that have been attributed earlier to the stronger acceptor capacity of the central oxyallyl ring. We have synthesized croconates with stronger donating groups as the side rings. The optical absorption is in the range of 400−500 nm. Comparison of the electron CT in these molecules with croconates absorbing in the NIR (above 700 nm) using SAC-CI methods, it is seen that the CT is smaller in the latter type of molecules. The diradical nature on the other hand is larger for the NIR croconates strongly supporting the observation that the NIR absorption has a correlation to the diradical character. The nonresonant NLO activity (γ) is determined using DFWM techniques at 800 nm. We obtain large $\chi^{(3)}$ values in both DMF and $CHCl_3$, and ultrafast optical response is also observed. We also determined the γ values in the solvent and find them to be very large in magnitude and negative in sign. These values are larger than the nonresonant values of similar squaraines reported in the literature. The larger γ value is attributed to the larger oxyallyl ring directly and indirectly to the diradical character in the case of croconates. The large γ values and tunable absorption maxima indicates that these dyes are promising molecular materials. We conclude that with a noncentrosymmetric structure, tunable NIR absorption, and larger γ values, these less studied croconate dyes are more interesting and will have a major role to play than the widely reported centrosymmetric squaraines as molecular materials.

Acknowledgment. We are thankful to DST, New Delhi for the funding of this project. We are also very much thankful to The Director, IICT and to The Head, Inorganic chemistry Division, IICT for their constant support in this work. Ch.P. thanks DST for the fellowship, and K.Y. and R.S.S.K. thank CSIR for the fellowship.

Supporting Information Available: This material is available free of charge via the Internet at http://pubs.acs.org.

References and Notes

(1) *Introduction to Nonlinear Optical Effects in Molecules and Polymers*; Prasad, P. N., Williams, D. J., Ed.;Wiley: New York, 1991.

(2) *Conjugated Polymers: The Novel Science and Technology of Highly Conducting and Nonlinear Optically Active materials*; Bredas, J. L., Silbey, R. J., Eds.; Kluwer: Dordrecht, Netherlands, 1991.

(3) Williams, D. J. *Angew. Chem., Int. Ed. Engl.* **1984**, *23*, 690.

(4) (a) Kanis, D. R.; Ratner, M. A.; Marks, T. J. *Chem. Rev.* **1994**, *94*, 195. (b) Zyss, J.; Ledoux, I. *Chem. Rev.* **1994**, *94*, 77.

(5) *Nonlinear Optical Materials. Theory and Modeling*; Karna, S. P., Yeates, A. T., Eds.; ACS Symposium Series 628, American Chemical Society: Washington, DC, 1996.

(6) Lindsay, G. A. Singer, K. D. In *Polymers for Second-Order Nonlinear Optics*; ACS Symposium Series 601,Amerian Chemical Society: Washington, DC, 1995.

(7) (a) *Molecular Nonlinear Optics: Materials, Physics, and Devices*; Zyss, J., Ed.; Academic Press: Boston, MA, 1993. (b) Sutherland, R. L. *Handbook of Nonlinear Optics*; Dekker: New York, 1996.

(8) (a) Verbiest, T.; Houbrechts, S.; Kauranen, M.; Clays, K.; Persoons, A. *J. Mater. Chem.* **1997**, *7*, 2175. (b) Verbiest, T.; Clays, K.; Samyn, C.; Wolff, J.; Reinhoudt, D.; Persoons, A. *J. Am. Chem. Soc.* **1994**, *116*, 9320. (c) Bredas, J. L.; Meyers, F.; Pierce, B. M.; Zyss, J. *J. Am. Chem. Soc.* **1992**, *114*, 4928. (d) Verbiest, T.; Clays, K.; Persoons, A.; Meyers, F.; Bredas, J. L. *Opt. Lett.* **1993**, *18*, 525.

(9) *Nonlinear Optical Properties of Organic Molecules and Crystal*; Chemla, D. S., Zyss, J., Eds.; Academic Press: Orlando, FL, 1987; vols. *1* and *2*.

(10) *Nonlinear Optics*; Boyd, R. W., Ed.; Academic Press: New York, 1992.

(11) Bredas, J. L.; Adant, C.; Tackx, P.; Persoons, A.; Pierce, B. M. *Chem. Rev.* **1994**, *94*, 243, and references cited therein.

(12) Nakano, M.; Kishi, R.; Ohta, S.; Takebe, A.; Takahashi, H.; Furukawa, S.; Takashi, K.; Morita, Y.; Nakasuji, K.; Yamaguchi, K.; Kamada, K.; Ohta, K.; Champagne, B.; Botek, E. *J. Chem. Phys.* **2006**, *125*, 74113.

(13) (a) Nakano, M.; Takashi, K.; Kamada, K.; Ohta, K.; Kishi, R.; Ohta, S.; Nakagawa, N.; Takahashi, H.; Furukawa, S.; Morita, Y.; Nakasuji, K.; Yamaguchi, K. *Chem. Phys. Lett.* **2006**, *418*, 142. (b) Ohta, S.; Nakano, M.; Takashi, K.; Kamada, K.; Ohta, K.; Kishi, R.; Nakagawa, N.; Champagne, B.; Botek, E.; Umezaki, S.; Takebe, A.; Takahashi, H.; Furukawa, S.; Morita, Y.; Nakasuji, K.; Yamaguchi, K. *Chem. Phys. Lett.* **2006**, *420*, 432. (c) Nakano, M.; Nakagawa, N.; Ohta, S.; Kishi, K.; Takashi, K.; Kamada, K.; Ohta, K.; Champagne, B.; Botek, E.; Takahashi, H.; Furukawa, S.; Morita, Y.; Nakasuji, K.; Yamaguchi, K. *Chem. Phys. Lett.* **2006**, *429*, 174.

(14) (a) Srinivas, K.; Prabhakar, Ch.; Lavanya Devi, C.; Yesudas, K.; Bhanuprakash, K.; Jayathritha Rao, V. *J. Phys. Chem. A* **2007**, *111*, 3378. (b) Anup, T.; Srinivas, K.; Prabhakar, Ch,.; Bhanuprakash, K.; Jayathirtha Rao, V. *Chem. Phys. Lett.* **2008**, *454*, 36. (c) Fabian, J. *Chem. Rev.* **1992**, *92*, 1197–1228.

(15) (a) Yesudas, K.; Bhanuprakash, K. *J. Phys. Chem. A* **2007**, *111*, 1943. (b) Prabhakar, Ch.; Krishna Chaitanya, G.; Sitha, S.; Bhanuprakash, K.; Jayathritha Rao, V. *J. Phys. Chem. A.* **2005**, *109*, 2614.

(16) (a) Prabhakar, Ch.; Yesudas, K.; Krishna Chaitanya, G.; Sitha, S.; Bhanuprakash, K.; Jayathritha Rao, V. *J. Phys. Chem. A.* **2005**, *109*, 8604. (b) Yesudas, K.; Krishna Chaitanya, G.; Prabhakar, Ch.; Bhanuprakash, K.; Jayathritha Rao, V. *J. Phys. Chem. A.* **2006110**, 11717.

(17) (a) Cariati, E.; Forni, A.; Biella, S.; Metrangolo, P.; Meyer, F.; Resnati, G.; Righetto, S.; Tordina, E.; Ugoa, R. *Chem. Commun.* **2007**, 2590. (b) Dragonetti, C.; Righetto, S.; Roberto, D.; Ugo, R.; Valore, A.; Fantacci, S.; Sgamellotti, A.; De Angelis, F. *Chem. Commun.* **2007**, 4116. (c) Sanguinet, L.; Williams, J. C.; Yang, Z.; Twieg, R. J.; Mao, G.; Singer, K. D.; Wiggers, G.; Petschek, R. G. *Chem. Mater.* **2006**, *18*, 4259. (d) Cheng, Y-J.; Luo, J.; Hau, S.; Bale, D. H.; Kim, T-D.; Shi, Z.; Lao, D. B.; Tucker, N. M.; Tian, Y.; Dalton, L. R.; Reid, P. J.; Jen, A. K-Y. *Chem. Mater.* **2007**, *19*, 1154.

(18) (a) Halter, M.; Liao, Y.; Plocinik, R. M.; Coffey, D. C.; Bhattacharjee, S.; Mazur, U.; Simpson, G. J.; Robinson, B. H.; Keller, S. L. *Chem. Mater.* **2008**, *20*, 1778. (b) Faccini, M.; Balakrishnan, M.; Diemeer, M. B. J.; Hu, Z-P.; Clays, K.; Asselberghs, I.; Leinse, A.; Driessen, A.; Reinhoudt, D. N. and Verboom, W. *J. Mater. Chem.* **2008**,DOI: 10.1039/b801728j. (c) David, K. S.; Hemeryck, A.; Tancrez, N.; Toupet, L.; Williams, J. A. G.; Ledoux, I.; Zyss, J.; Boucekkine, A.; Guegan, J-P.; Bozec, H. L.; Maury, O. *J. Am. Chem. Soc.* **2006**, *128*, 12243. (d) Cariati, E.; Macchi, R.; Roberto, D.; Ugo, R.; Galli, S.; Casati, N.; Macchi, P.; Sironi, A.; Bogani, L.; Caneschi, A.; Gatteschi, D. *J. Am. Chem. Soc.* **2007**, *129*, 9410.

(19) (a) Lamere, J. F.; Lacroix, P. G.; Farfan, N.; Rivera, J. M.; Santillanc, R.; Nakatani, K. *J. Mater. Chem.* **2006**, *16*, 2913. (b) Schmidt, K.; Barlow, S.; Leclercq, A.; Zojer, E.; Jang, S-H.; Marder, S. R.; Jen, A. K.-Y.; Bredas, J-L. *J. Mater. Chem.* **2007**, *17*, 2944. (c) Zrig, S.; Koeckelberghs, G.; Verbiest, T.; Andrioletti, B.; Rose, E.; Persoons, A.; Asselberghs, I.; Clays, K. *J. Org. Chem.* **2007**, *72*, 5855. (d) Li, Z.; Chen, Z.; Xu, S.; Niu, L.; Zhang, Z.; Zhang, F.; Kasatani, K. *Chem. Phys. Lett.* **2007**, *447*, 110. (e) Yuan, Z.; Entwistle, C. D.; Collings, J. C.; Albesa-Jove, D.; Batsanov, A. S.; Howard, J. A. K.; Taylor, N. J.; Kaiser, H. M.; Kaufmann, D. E.; Poon, S-Y.; Wong, W-Y.; Jardin, C.; Fathallah, S.; Boucekkine, A.; Halet, J-F.; Marder, T. B. *Chem.—Eur. J.* **2006**, *12*, 2758.

(20) (a) Tatsuura, S.; Tian, M.; Furuki, M.; Sato, Y.; Iwasa, I.; Mitsu, H. *Appl. Phys. Lett.* **2004**, *84*, 1450. (b) Tatsuura, S.; Mastubara, T.; Tian, M.; Mitsu, H.; Iwasa, I.; Sato, Y.; Furuki, M. *Appl. Phys. Lett.* **2004**, *85*, 540.

(21) (a) Li, Z.; Song, X.; Lei, H.; Xin, H.; Lihong, N.; Zihui, C.; Zhi, Z.; Fushi, Z.; Kazuo, K. *Chem. Phys. Lett.* **2007**, *441*, 123. (b) LI, Z-Y.; Jin, Z-H.; Kasatani, K.; Okamoto, H. *Chin. Phys. Lett.* **2005**, *22*, 2282. (c) Dirk, C. W.; Herndon, W. C.; Cervantes-Lee, F.; Selnau, H.; Martinez, S.; Kalamegham, P.; Tan, A.; Campos, G.; Velez, M.; Zyss, J.; Ledoux, I.; Cheng, L-T. *J. Am. Chem. Soc.* **1995**, *117*, 2214. (d) Tran, K.; Scott, G. W.; Funk, D. J.; Moore, D. S. *J. Phys. Chem.* **1996**, *100*, 11863. (e) Andrews, J. H.; Khaydarov, J. D. V.; Singer, K. D. *Opt. Lett.* **1994**, *19*, 984.

(22) (a) Srinivas, K.; Sitha, S.; Jayathirtha Rao, V.; Bhanuprakash, K.; Ravikumar, K. *J. Mater. Chem.* **2006**, *16*, 496. (b) Srinivas, K.; Sitha, S.; Jayathirtha Rao, V.; Bhanuprakash, K.; Ravikumar, K.; Philip Anthony, S.; Radhakrishnan, T. P. *J. Mater. Chem.* **2005**, *15*, 965.

(23) (a) Srinivas, K.; Sitha, S.; Jayathirtha Rao, V.; Bhanuprakash, K. *Opt. Mater.* **2006**, *28*, 1006. (b) Sitha, S.; Srinivas, K.; Raghunath, P.; Bhanuprakash, K.; Jayathirtha Rao, V. *J. Mol. Struc. (Theochem)* **2005**, *728*, 57. (c) Sitha, S.; Laxmikanth Rao, J.; Bhanuprakash, K.; Choudary, B. M. *J. Phys.Chem. A* **2001**, *105*, 8727.

(24) (a) Sai Santosh Kumar, R.; Venugopal Rao, S.; Giribabu, L.; Narayana Rao, D. *Chem. Phys. Lett.* **2007**, *447*, 274. (b) Patil, P. S.; Dharmaprakash, S. M.; Ramakrishna, K.; Fun, H-K.; Sai Santosh Kumar, R.; Narayana Rao, D. *J. Cryst. Growth* **2007**, *303*, 520. (c) Venugopal Rao, S.; Naga Srinivas, N. K. M.; Narayana Rao, D.; Giribabu, L.; Bhaskar, G. M.; Philip, R.; Ravindra Kumar, G. *Opt. Commun.* **2000**, *182*, 255.

(25) Langhals, H. *Angew Chem, Int. Ed.* **2003**, *42*, 4286.

(26) (a) Li, Z.; Jin, Z-H.; Kasatani, K.; Okamoto, H. *Physica B.* **2006**, *382*, 229. (b) Li, Z.; Jin, Z-H.; Kasatani, K.; Okamoto, H.; Takenaka, S. *Jpn. J. Appl. Phys.* **2005**, *44*, 4956.

(27) (a) Fatiadi, J. A.; Isbell, S. H.; Sager, F. W. *J. Res. Nat. Bur. Stand. (U.S.)* **1963**, *67A*, 153. (b) Yamada, K.; Hirata, Y. *Bull. Chem. Soc. Jpn.* **1958**, *31*, 550.

(28) Park, S. Y.; Jun, K.; Oh, S-W. *Bull. Korean Chem. Soc.* **2005**, *26*, 428.

(29) Frisch, M. J.; Trucks, G. W.; Schlegel, H. B.; Scuseria, G. E.; Robb, M. A.; Cheeseman, J. R.; Montgomery, J. A., Jr.; Vreven, T.; Kudin, K. N.; Burant, J. C.; Millam, J. M.; Iyengar, S. S.; Tomasi, J.; Barone, V.; Mennucci, B.; Cossi, M.; Scalmani, G.; Rega, N.; Petersson, G. A.; Nakatsuji, H.; Hada, M.; Ehara, M.; Toyota, K.; Fukuda, R.; Hasegawa, J.; Ishida, M.; Nakajima, T.; Honda, Y.; Kitao, O.; Nakai, H.; Klene, M.; Li, X.; Knox, J. E.; Hratchian, H. P.; Cross, J. B.; Adamo, C.; Jaramillo, J.; Gomperts, R.; Stratmann, R. E.; Yazyev, O.; Austin, A. J.; Cammi, R.; Pomelli, C.; Ochterski, J. W.; Ayala, P. Y.; Morokuma, K.; Voth, G. A.; Salvador, P.; Dannenberg, J. J.; Zakrzewski, V. G.; Dapprich, S.; Daniels, A. D.; Strain, M. C.; Farkas, O.; Malick, D. K.; Rabuck, A. D.; Raghavachari, K.; Foresman, J. B.; Ortiz, J. V.; Cui, Q.; Baboul, A. G.; Clifford, S.; Cioslowski, J.; Stefanov, B. B.; Liu, G.; Liashenko, A.; Piskorz, P.; Komaromi, I.; Martin, R. L.; Fox, D. J.; Keith, T.; Al-Laham, M. A.; Peng, C. Y.; Nanayakkara, A.; Challacombe, M.; Gill, P. M. W.; Johnson, B.; Chen, W.; Wong, M. W.; Gonzalez, C.; Pople, J. A.; *Gaussian 03*, revision 01; Gaussian, Inc.: Wallingford, CT, 2004.

(30) Stratmann, R. E.; Scuseria, G. E.; Frisch, M. J. *J. Chem. Phys.* **1998**, *109*, 8218. (b) Hirata, S.; Lee, T. J.; Head-Gordon, M. *J. Chem. Phys.* **1999**, *111*, 8904. (c) Bauernschmitt, R.; Haŝer, M.; Treutler, O.; Ahlichs, R. *Chem. Phys. Lett.* **1997**, *264*, 573.

(31) (a) Nakajima, T.; Nakatsuji, H. *Chem. Phys. Lett.* **1997**, *280*, 79. (b) Ishida, M.; Toyota, K.; Ehara, M.; Nakatsuji, H. *Chem. Phys. Lett.* **2001**, *347*, 493. (c) Nakajima, T.; Nakatsuji, H. *Chem. Phys. Lett.* **1999**, *242*, 177. (d) Nakajima, T.; Nakatsuji, H. *Chem. Phys. Lett.* **1999**, *300*, 1. (e) Wan, J.; Ehara, M.; Hada, M.; Nakatsuji, H. *J. Chem. Phys.* **2000**, *113*, 5245. (f) Wan, J.; Hada, M.; Ehara, M.; Nakatsuji, M. *J. Chem. Phys.* **2001**, *114* (2), 842. (g) Nakatsuji, H. *ACH - Models Chem.* **1992**, *129*, 719. (h) Nakatsuji, H. In *Computational Chemistry - Reviews of Current Trends*; Leszczynski, J., Ed.; World Scientific: River Edge, NJ, 1997; Vol. 2.

(32) (a) Wirz, J. *Pure Appl. Chem.* **1984**, *56*, 1289. (b) Dohnert, D.; Koutecky, J. *J. Am. Chem. Soc.* **1980**, *102*, 1790.

(33) Simard, T. P.; Yu, J. H.; Zebrowski-Young, J. M.; Haley, N. F.; Detty, M. R. *J. Org. Chem.* **2000**, *65*, 2236.

(34) Orr, J.; Ward, J. F. *Mol. Phys.* **1971**, *20*, 513.

(35) Kamada, K.; Ueda, M.; Nagao, H.; Tawa, K.; Takushi, S.; Shmizu, Y.; Ohta, K. *J. Phys. Chem. A* **2000**, *104*, 4723, and references cited therein.

(36) Marek, S.; Anna, S.; Barry, L-D.; Zhenan, B.; Luping, Y.; Bing, H.; Ullrich, S. *J. Opt. Soc. Am. B* **1998**, *15*, 817.

(37) Mingtang, Z.; Yiping, C.; Marek, S.; Prasad, P. N.; Marilyn, R. U.; Bruce, A. R. *J. Chem. Phys.* **1991**, *95*, 3991.